



Cite this: *New J. Chem.*, 2016, 40, 10554

Received (in Montpellier, France)
5th September 2016,
Accepted 9th November 2016

DOI: 10.1039/c6nj02717b

www.rsc.org/njc

Porous coordination polymer coatings fabricated from $\text{Cu}_3(\text{BTC})_2 \cdot 3\text{H}_2\text{O}$ with excellent superhydrophobic and superoleophilic properties

Wen Meng,^a Zhijuan Feng,^a Feng Li,^{*a} Taohai Li^a and Wei Cao^b

A rare example in which the wettability of porous coordination polymer coatings fabricated from $\text{Cu}_3(\text{BTC})_2 \cdot 3\text{H}_2\text{O}$ was investigated. The sample exhibited excellent superhydrophobicity and superoleophilicity. Furthermore, the superhydrophobic $\text{Cu}_3(\text{BTC})_2 \cdot 3\text{H}_2\text{O}$ -coated surfaces showed excellent corrosion resistance and long-term stability. These properties make this metal–organic framework (MOF) material attractive for future applications as self-cleaning and oil-absorbing materials.

Introduction

It is well-known that, over the last few decades, inspired by biological organisms with special surface wettability, especially the self-cleaning properties of lotus leaves,^{1,2} people have paid high attention to the design of artificial superhydrophobic surfaces with self-cleaning effects. Such superhydrophobic surfaces typically have a high water contact angle ($\text{CA} > 150^\circ$) and a low contact angle hysteresis ($\text{CAH} < 10^\circ$).³ Recently, solid surfaces possessing both superhydrophobicity and superoleophilicity have attracted great interest in fundamental research as well as practical applications in the fields of self-cleaning and industrial oily wastewater treatment.^{4,5}

Basically, the hydrophobicity of a solid surface is governed by both the topology and the chemistry of the surface.⁶ Among various factors, surface roughness and surface energy are the predominant factors that determine the wettability.⁷ In general, a superhydrophobic surface can be obtained by creating a rough surface first and then modifying the rough surface with a special low surface energy material. We know that a surface with a porous structure can increase the surface roughness dramatically and trap a large quantity of air within it, which may lead to superhydrophobic behaviour, because microscopic pockets of air appear underneath the liquid droplet, resulting in a composite interface (Cassie model).⁸ Therefore, materials with a porous structure are helpful in the construction of a rough surface.

MOFs are a class of highly porous crystalline materials that have attracted a high level of attention in inorganic and

materials chemistry due to their highly predictable topologies, controllable structural flexibility, and various modifiable functionalities.^{9,10} These unique advantages allow MOFs to be applied in diverse areas. To date, a wide range of research related to the application of MOFs such as in catalysis, gas storage, photoluminescence and magnetism has been reported.^{11–16} However, little has been done to fabricate superhydrophobic surfaces based on MOFs although great progress has been made in the preparation of superhydrophobic materials. In fact, MOF materials with abundantly porous structures and functional surface groups offer much potential for the introduction of hydrophobic properties within the materials. Moreover, the surface roughness can be controlled according to people's wishes by chemically tailoring the porosity of the MOFs to achieve an ideal wettability.

$\text{Cu}_3(\text{BTC})_2 \cdot 3\text{H}_2\text{O}$ (BTC = benzene-1,3,5-tricarboxylate), known as HKUST-1, is one of the most well-known porous metal organic frameworks that possess large surface areas and pore volume. Unfortunately, the majority of work on it has by far been focused on storage and separation of gases, heterogeneous catalysis and sensing.^{17–19} Reports on the wettability of coordination polymer coatings fabricated from $\text{Cu}_3(\text{BTC})_2 \cdot 3\text{H}_2\text{O}$ have been scarce up to now. Herein we report on the wettability of the modified- $\text{Cu}_3(\text{BTC})_2 \cdot 3\text{H}_2\text{O}$ coatings prepared on a glass substrate by a simple drop-coating procedure. The as-prepared $\text{Cu}_3(\text{BTC})_2 \cdot 3\text{H}_2\text{O}$ coatings exhibit excellent superhydrophobic and superoleophilic properties, which suggest promising applications of the MOFs as self-cleaning and oil-absorbing materials. $\text{Cu}_3(\text{BTC})_2 \cdot 3\text{H}_2\text{O}$ was prepared by a solvothermal reaction. Superhydrophobic surfaces were prepared *via* a facile drop-casting method. And the preparation process needs neither specialized reagents and equipment nor sophisticated procedures. Compared with other methods described in the literature for the preparation of superhydrophobic surfaces, the presented method is much simpler and cheaper.

^a College of Chemistry, Key Lab of Environment Friendly Chemistry and Application in Ministry of Education, Xiangtan University, Xiangtan, China.

E-mail: fengli_xtu@hotmail.com; Fax: +86-731-58292251; Tel: +86-731-58292206

^b Department of Physics and Chemistry, University of Oulu, P.O. Box 3000, FIN-90014, Finland



Experimental

Materials

Copper(II) chloride dihydrate, 1,3,5-benzene tricarboxylic acid (H_3BTC), sodium hydroxide, anhydrous ethanol, stearic acid and 1H,1H,2H,2H-perfluorodecyltriethoxysilane (PFOTS) were purchased from commercial suppliers and used without further purification. The glass substrate was obtained locally, and was cut into smaller 1.0 cm \times 1.0 cm squares before usage. Then the glass was further purified by ultrasonic washing with acetone, anhydrous ethanol and deionized water for 15 min, sequentially, and then dried in a clean oven at 60 °C for 1 h.

$Cu_3(BTC)_2 \cdot 3H_2O$ synthesis and characterization

$Cu_3(BTC)_2 \cdot 3H_2O$ was prepared by a solvothermal reaction. First, $CuCl_2 \cdot 2H_2O$ (4.1 mmol, 699 mg) was dissolved in 13.5 mL of deionized water, and then mixed with H_3BTC (2.7 mmol, 567 mg) dissolved in 13.5 mL of ethanol. The pH value of the mixed solution was adjusted to 2.0 with 0.1 M NaOH solution, and then the mixture was stirred for 30 min at room temperature. The resulting mixture was transferred into a 45 mL Teflon-lined autoclave, and heated at 140 °C for 24 h. After slow cooling to room temperature, the obtained blue powder was filtered, washed with deionized water (3×10 mL) and ethanol (3×10 mL), and then dried overnight in the oven at 70 °C to give 0.54 g $Cu_3(BTC)_2 \cdot 3H_2O$ with a yield based on Cu of 59%.

The composition and crystal structure of the $Cu_3(BTC)_2 \cdot 3H_2O$ samples were determined by powder XRD measurement using a MiniFlex II diffractometer (continuous, 30 kV, 15 mA, increment = 0.02°). The surface morphology of the $Cu_3(BTC)_2 \cdot 3H_2O$ -coated surfaces and chemical composition of the as-synthesized $Cu_3(BTC)_2 \cdot 3H_2O$ samples were characterized on a scanning electron microscope (SEM, JSM-6490-LV) equipped with an energy dispersive X-ray spectrometer (EDS). FTIR spectra were recorded using a Fourier transform spectrometer (Nicolet 6700) in the region of 4000–500 cm^{-1} . N_2 adsorption–desorption isotherms were measured at liquid nitrogen temperature using a sorption analyzer (Micromeritics, Tristar II 3020). Prior to the measurements, the samples were outgassed at 150 °C for 8 h. The BET specific surface area was evaluated in the p/p_0 range of 0.05–0.35. Water contact angle (CA) measurements were carried out on a Ramé-hart model p/n 250-F1. Water droplets at a pH value of 7 (5 μ L) were carefully dropped onto the surfaces, and the average value of five measurements obtained at different positions in the samples was used as the final contact angle. The sliding angle was measured by tilting the sample stage from 0° to higher angles and then a water droplet was placed on the inclined surfaces. When the droplet rolled off the surface, the angle of the sample stage was recorded as the sliding angle.

Fabrication of superhydrophobic surfaces

Superhydrophobic surfaces were prepared *via* a facile dip-coating method. Typically, the as-prepared $Cu_3(BTC)_2 \cdot 3H_2O$ samples were ultrasonically dispersed in ethanol to form a uniform suspension, and then several drops of the suspension were dropped onto the glass substrate. When the ethanol was

completely evaporated at ambient temperature, a thin film was formed on the surface of the glass substrate. Finally, in order to reduce the surface energy of the fabricated structures, the film on the glass substrate was modified by stearic acid and PFOTS individually. The treatment with stearic acid was conducted by adding a 10 mM stearic acid solution of *n*-hexane. Firstly, 10 mM of stearic acid solution was prepared using *n*-hexane as the solvent and the configured solution was preserved in a brown volumetric flask. Secondly, after the film on the glass substrate was air dried, a dropper was used to fetch some of the solution, dropping it onto the film until all of the film surface was wet. Then, the $Cu_3(BTC)_2 \cdot 3H_2O$ -coated glasses were dried for 24 h in an air atmosphere at ambient temperature. Similarly, the treatment with PFOTS was conducted by adding a methanol solution of 2% (v/v) PFOTS (as a contrast, $Cu_3(BTC)_2 \cdot 3H_2O$ coatings on glass substrates without further modification were also prepared in this study). Finally, the porous superhydrophobic $Cu_3(BTC)_2 \cdot 3H_2O$ coatings were fabricated on a glass surface by the single-step procedure.

Results and discussion

$Cu_3(BTC)_2 \cdot 3H_2O$ was synthesized from the reaction of $CuCl_2 \cdot 2H_2O$ and H_3BTC by a simple solvothermal reaction. The pH value of the mixed solution was adjusted to 2.0 with a 0.1 M NaOH solution. In order to investigate the superhydrophobic and superoleophilic properties of the coordination polymer, a facile drop-casting method was used to prepare the $Cu_3(BTC)_2 \cdot 3H_2O$ coatings. Stearic acid and PFOTS were used to modify the films on the glass substrates in order to reduce the surface energy of the fabricated structures.

The X-ray power diffraction (PXRD) pattern of the as-synthesized $Cu_3(BTC)_2 \cdot 3H_2O$ powder is shown in Fig. 1a, which is in agreement with the simulated one generated on the basis of single crystal X-ray data obtained from previous literature.²⁰ It strongly suggests that the crystalline MOF sample is isostructural to the previously reported $Cu_3(BTC)_2 \cdot 3H_2O$. The N_2 adsorption/desorption isotherm of $Cu_3(BTC)_2 \cdot 3H_2O$ (Fig. 1b) displays type I behavior, which is characteristic of a micropore structure, with a BET surface area of 1323 $m^2 g^{-1}$ and a pore volume of 0.49 $cm^3 g^{-1}$. The BET surface area was fairly close to that reported by Wang *et al.*, but the pore volume was slightly lower than the reported value (0.658 $cm^3 g^{-1}$).²¹ However, the results were much higher than the values obtained by Chui *et al.*²² A detailed report on specific surface area and pore volume values published in different articles^{23–26} is shown in Table 1. The chemical composition of the sample was characterized by energy-dispersive X-ray spectroscopy (EDS) analysis (Fig. 2), which reveals that the main elements are C, O and Cu for $Cu_3(BTC)_2 \cdot 3H_2O$.

Fig. 3A(a) is the generated equation for $Cu_3(BTC)_2 \cdot 3H_2O$ and Fig. 3A(b) is the molecular stick model diagram of $Cu_3(BTC)_2 \cdot 3H_2O$. The C, O, H and Cu atoms were represented by gray spheres, bright red spheres, white spheres and blue spheres, respectively. From the equation it can be seen that three copper ions reacted with three carboxyls of the H_3BTC and formed Cu–O bonds.^{27,28} The FTIR spectrum of the sample is presented



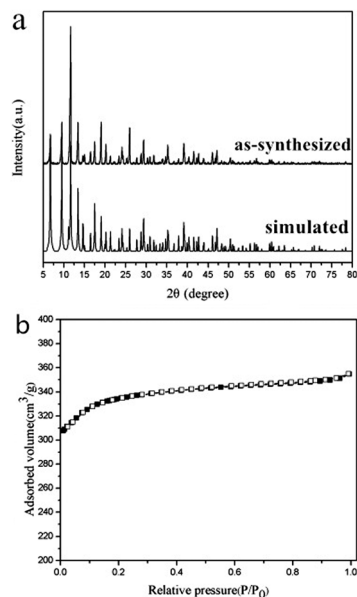


Fig. 1 (a) XRD patterns and (b) N_2 physisorption study (77 K) for $Cu_3(BTC)_2 \cdot 3H_2O$, where closed and open symbols are for the adsorption branch and desorption branch, respectively.

Table 1 Comparison of surface area and pore volumes for different Cu-BTC samples cited in the literature

Ref.	BET surface area ($m^2 g^{-1}$)	Pore volume ($cm^3 g^{-1}$)
Present work	1323	0.49
22	964, 1333 (different batches)	0.658
23	692.2	0.333
26	1482	0.828
27	1507	0.75
28	857, 1482 (different batches)	0.425, 0.753
29	1296	0.69
30	857, 1482 (different batches)	0.425, 0.753

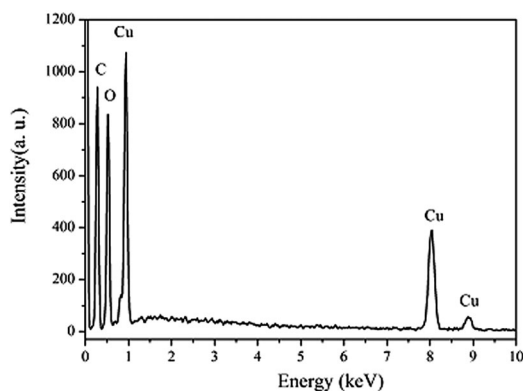


Fig. 2 EDS analysis of $Cu_3(BTC)_2 \cdot 3H_2O$.

in Fig. 3B. The broad absorption band centered around 3354 cm^{-1} is assigned to the O–H stretching vibration. The bands at 1615 , 1541 , 1443 and 1367 cm^{-1} are due to the presence of $-C(OCu)OCu$ metallic esters, indicating the bridging bidentate coordination state in the compounds.^{29,30} And the two bands at 727 and 759 cm^{-1} are attributed to metal Cu

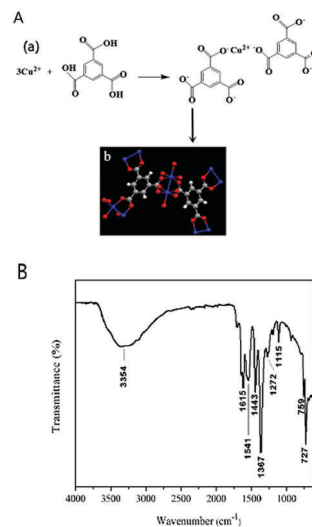


Fig. 3 (A) The structure of $Cu_3(BTC)_2 \cdot 3H_2O$; (B) the IR spectrum of $Cu_3(BTC)_2 \cdot 3H_2O$.

substitution of the carboxyl hydrogen on H_3BTC . In addition, the presence of absorption bands at 1272 and 1115 cm^{-1} can be considered as the C–O stretching vibration of small amounts of ethanol trapped within the porous net.³¹ The above results provide clear evidence of the formation of $Cu_3(BTC)_2 \cdot 3H_2O$.

The morphologies of the $Cu_3(BTC)_2 \cdot 3H_2O$ -coated surface before (Fig. 4a) and after surface modification by stearic acid and PFOTS (Fig. 4b and c) are mostly similar, presenting highly porous and rough structures formed by $1\text{--}2\text{ }\mu\text{m}$ granules. There are numerous pores formed by these particulates, which increased the surface roughness. This observation is consistent with the results obtained for the BET surface areas of $Cu_3(BTC)_2 \cdot 3H_2O$. It is reported that such surface structures can trap a large quantity of air within them so that it is difficult therefore for water droplets to penetrate into the pores.³² It can be discerned from the images at higher magnification in the insets of Fig. 4 that the randomly stacked clusters of particulates give rise to hierarchical structures with roughness at various length scales, which is favourable for the non-wetting properties.

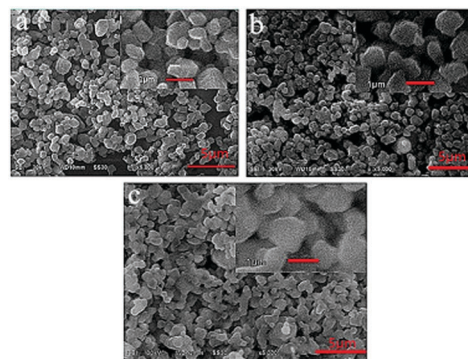


Fig. 4 SEM images of the as-prepared $Cu_3(BTC)_2 \cdot 3H_2O$ coatings: (a) without treatment; (b) treated with stearic acid; (c) treated with PFOTS. The corresponding high magnification SEM images are showed on the right upper part.



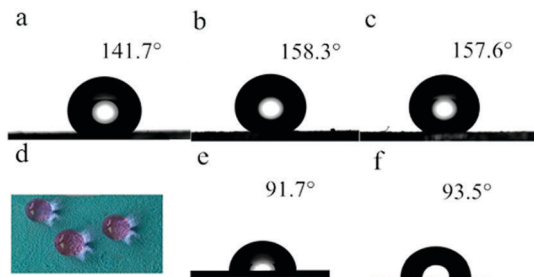


Fig. 5 (a) Profiles of water contact angles for surfaces without treatment, (b) treated with stearic acid and (c) treated with PFOTS, (d) a photograph of spherical water droplets on the surface treated with stearic acid, and (e) water contact angles on smooth glass surfaces modified by stearic acid and (f) modified by PFOTS.

As can be seen in Fig. 5a, the surface without modification has obtained a water contact angle of $141.7^\circ \pm 0.5^\circ$. After surface modification, the as-synthesized surfaces were demonstrated to be superhydrophobic, as shown in Fig. 5b and c. The $\text{Cu}_3(\text{BTC})_2$ -coated surfaces modified by stearic acid and PFOTS have a water contact angle of $158.3^\circ \pm 0.5^\circ$ and $157.6^\circ \pm 0.5^\circ$, respectively. Interestingly, the corresponding water sliding angles were $5^\circ \pm 1^\circ$ and $2^\circ \pm 1^\circ$, respectively (Fig. 6). Fig. 5d shows a photograph of spherical water droplets (water was colored with RhB) on the surface treated with stearic acid. The wetting behavior can be interpreted by the Cassie model shown in eqn (1):

$$\cos \theta' = f_1 \cos \theta - f_2 \quad (1)$$

Here, θ is the CA of a smooth glass surface modified by stearic acid or PFOTS with water contact angles of $91.7^\circ \pm 0.5^\circ$ and $93.5^\circ \pm 0.5^\circ$, respectively, as shown in Fig. 5e and f. θ' is the CA of a superhydrophobic $\text{Cu}_3(\text{BTC})_2$ -coated surface; f_1 and f_2 are the fractions of solid surface and air in a composite surface, respectively (*i.e.*, $f_1 + f_2 = 1$). The f_1 value of the superhydrophobic surface modified by stearic acid (or PFOTS) is calculated to be 0.074 (or 0.080), which indicates that surface structures with air trapped in the valleys between asperities are essential for the preparation of low-sliding-angle surfaces.³³

It is necessary to investigate the wettability of corrosive liquids on the superhydrophobic surface. Fig. 7c shows the relationship between pH values of water droplets and the contact angles on the as-synthesized porous superhydrophobic surface. The contact angles on the PFOTS-treated surface range from about 152.8° to 157.6° when the pH varied from 3 to 13. Only when the pH value is decreased to 1, did the contact angle show a larger fluctuation in the value but still reached about 139.9° . For the superhydrophobic surface treated with stearic acid, the fluctuation of the CA with pH is similar to that of the PFOTS-treated surface. The CA remained in the range of 150.5 – 158.3° when the pH increased from 3 to 11. The contact angle decreased to 134.5° for a pH value of 1 and 148.6° for a pH value of 13. However, the porous superhydrophobic surfaces all show superhydrophobic properties in the pH range from 3 to 11, indicating that the as-obtained $\text{Cu}_3(\text{BTC})_2 \cdot 3\text{H}_2\text{O}$ coatings on glass surfaces possess an excellent hydrophobic property not

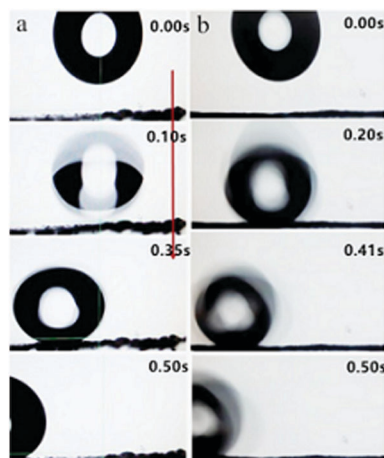


Fig. 6 Sliding behavior of a water droplet on the superhydrophobic surfaces (drop weight, 5 mg): (a) a surface treated with stearic acid, tilt angle of the surface: 5° ; (b) a surface treated with PFOTS, tilt angle of the surface: 2° . These pictures were taken from video clips.

only for pure water but also corrosive liquids such as acidic and basic aqueous solutions. To further evaluate the corrosion resistance of the surfaces, we also measured the contact angles of a 5 wt% NaCl aqueous solution on the superhydrophobic surfaces, giving a value of $153.6^\circ \pm 0.5^\circ$ for the surface treated with stearic acid and $154.2^\circ \pm 0.5^\circ$ for the PFOTS-treated surface (Fig. 7a).

Furthermore, the superhydrophobic surfaces were exposed to the ambient air for 4 months, and the contact angles on the surfaces modified by stearic acid and PFOTS were $156.8^\circ \pm 0.5^\circ$ and $157.4^\circ \pm 0.5^\circ$, respectively, retaining superhydrophobicity with the contact angles remaining almost unchanged (Fig. 7b). The results suggest that the superhydrophobic surfaces have good long-term stability in air.

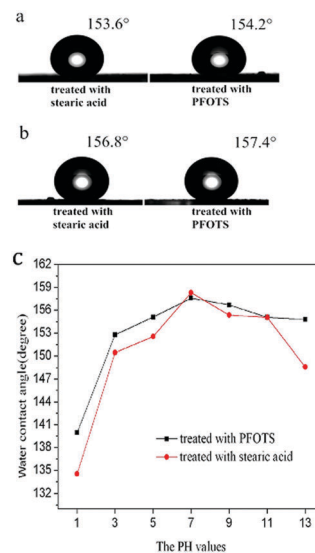


Fig. 7 (a) Profiles of the contact angles of a 5 wt% NaCl aqueous solution on the obtained superhydrophobic surfaces; (b) profiles of the water contact angles on the superhydrophobic surface after standing for 4 months; (c) the relationship between the pH values of water droplets and the contact angles on the modified superhydrophobic surfaces.



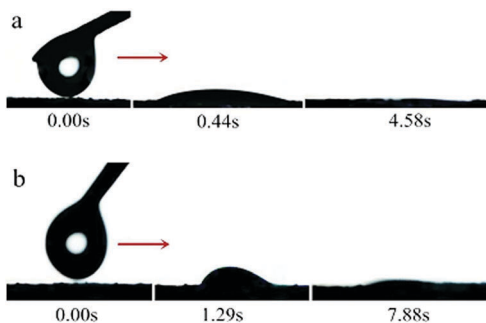


Fig. 8 The adsorption behavior of an oil droplet on the as-obtained $\text{Cu}_3(\text{BTC})_2$ coatings on glass surfaces: (a) treated with stearic acid; (b) treated with PFOTS. These pictures were taken from video clips.

The as-obtained superhydrophobic surfaces were confirmed to possess simultaneous superhydrophobicity and superoleophilicity. When a *n*-octane droplet (5 μL) was dropped onto the surface treated with stearic acid (Fig. 8a), the *n*-octane spread quickly on the coating and was absorbed thoroughly within about 4 s. Similarly, the PFOTS-treated surface could absorb the *n*-octane droplet within about 7 s (Fig. 8b), exhibiting outstanding superoleophilicity.

As is well known, MOFs are crystalline, inorganic–organic hybrid porous materials. The presence of carboxylate-based ligands in $\text{Cu}_3(\text{BTC})_2$ may contribute to its affinity for oil. On the whole, the surface chemical composition and geometrical structure of $\text{Cu}_3(\text{BTC})_2$ induce its unique wettability towards water and oil, which not only indicates that it can be used for self-cleaning and oil-absorbing materials, but also paves the way for its application in oil/water separation. It should be noted that compared to their traditional porous inorganic (zeolites, phosphates, and oxides) or organic (activated carbons) counterparts, MOFs are unique in terms of their good crystallinity, designable porosity, and structural flexibility. These unique advantages give rise to the possibility of the synthesis of new types of tailored porous materials with specific wettability.

Conclusions

In conclusion, we have developed a simple and low cost dip-coating method to fabricate porous $\text{Cu}_3(\text{BTC})_2 \cdot 3\text{H}_2\text{O}$ coatings on glass surfaces with the particular wettability of superhydrophobicity and superoleophilicity. Moreover, the modified surfaces have a low water sliding angle, and water droplets could easily roll off the modified surfaces. This valuable finding provides us with new perspectives and possibilities for preparing neoteric interfacial materials. Further studies will be performed to design appropriate functional membranes based on MOFs of $\text{Cu}_3(\text{BTC})_2 \cdot 3\text{H}_2\text{O}$ in order to realize the application of oil/water separation.

Acknowledgements

The authors acknowledge with thanks the financial support of the Provincial Natural Science Foundation of Hunan, China

(2015JJ2138), the Open Project Program of State Key Laboratory of Structural Chemistry, China (No. 20150018) and the National Natural Science Foundation of China (21601149) and the Oulu University Strategic Grant. T. Li acknowledges the Oulu University Short-term International Research Visit grant during his stay in Finland.

Notes and references

- B. Bhushan, Y. C. Jung and K. Koch, *Langmuir*, 2009, **25**, 3240–3248.
- K. Koch, H. F. Bohn and W. Barthlott, *Langmuir*, 2009, **25**, 14116–14120.
- W. Guo, Q. Zhang, H. B. Xiao, J. Xu, Q. T. Li, X. H. Pan and Z. Y. Huang, *Appl. Surf. Sci.*, 2014, **314**, 408–414.
- L. Wu, J. P. Zhang, B. C. Li and A. Q. Wang, *J. Colloid Interface Sci.*, 2014, **413**, 112–117.
- M. Zhang, C. Y. Wang, S. L. Wang and J. Li, *Carbohydr. Polym.*, 2013, **97**, 59–64.
- L. Feng, S. H. Li, Y. S. Li, H. J. Li, L. J. Zhang, J. Zhai, Y. L. Song, B. Q. Liu, L. Jiang and D. B. Zhu, *Adv. Mater.*, 2002, **14**, 24.
- N. Zhao, J. Xu, Q. D. Xie, L. H. Weng, X. L. Guo, X. L. Zhang and L. H. Shi, *Macromol. Rapid Commun.*, 2005, **26**, 1075–1080.
- C. Yang, U. Tartaglino and B. N. J. Persson, *Phys. Rev. Lett.*, 2006, **97**, 116103.
- J. L. C. Rowsell and O. M. Yaghi, *Microporous Mesoporous Mater.*, 2004, **73**, 3–14.
- H. Furukawa, K. E. Cordova, M. O’Keeffe and O. M. Yaghi, *Science*, 2013, **341**, 974.
- J. Y. Lee, O. K. Farha, J. Roberts, K. A. Scheidt, S. T. Nguyen and J. T. Hupp, *Chem. Soc. Rev.*, 2009, **38**, 1450–1459.
- Y. S. Xue, Y. He, L. Zhou, F. J. Chen, Y. Xu, H. B. Du, X. Z. You and B. Chen, *J. Mater. Chem. A*, 2013, **1**, 4525–4530.
- H. P. Jia, W. Li, Z. F. Ju and J. Zhang, *Inorg. Chem. Commun.*, 2007, **10**, 265–268.
- Z. Wang, X. Y. Li, L. W. Liu, S. Q. Yu, Z. Y. Feng, C. H. Tong and D. Sun, *Chem. – Eur. J.*, 2016, **22**, 6830.
- S. Yuan, Y. K. Deng and D. Sun, *Chem. – Eur. J.*, 2014, **20**, 10093.
- Z. H. Yan, X. Y. Li, L. W. Liu, S. Q. Yu, X. P. Wang and D. Sun, *Inorg. Chem.*, 2016, **55**, 1096.
- L. Hamon, E. Jolimaitre and G. D. Pirngruber, *Ind. Eng. Chem. Res.*, 2010, **49**, 7497–7503.
- N. Janssens, L. H. Wee, S. Bajpe, E. Breynaert, C. E. A. Kirschhock and J. A. Martens, *Chem. Sci.*, 2012, **3**, 1847–1850.
- J. Liu, F. X. Sun, F. Zhang, Z. Wang, R. Zhang, C. Wang and S. L. Qiu, *J. Mater. Chem.*, 2011, **21**, 3775–3778.
- M. Schlesingera, S. Schulze, M. Hietschold and M. Mehring, *Microporous Mesoporous Mater.*, 2010, **132**, 121–127.
- Q. M. Wang, D. Shen, M. Bülow, M. L. Lau, S. Deng, F. R. Fitch, N. O. Lemcoff and J. Semanscin, *Microporous Mesoporous Mater.*, 2002, **55**, 217.
- S. S.-Y. Chui, S. M. F. Lo, J. P. H. Charmant, A. G. Orpen and I. D. Williams, *Science*, 1999, **283**, 1148.
- J. Liu, J. T. Culp, S. Natesakhawat, B. C. Bockrath, B. Zande, S. G. Sankar, G. Garberoglio and J. K. Johnson, *J. Phys. Chem. C*, 2007, **111**, 9305.



- 24 J. L. C. Rowsell and O. M. Yaghi, *J. Am. Chem. Soc.*, 2006, **128**, 1304.
- 25 Y. Li and R. T. Yang, *AIChE J.*, 2008, **54**, 269.
- 26 P. Chowdhury, C. Bikkina, D. Meister, F. Dreisbach and S. Gumma, *Microporous Mesoporous Mater.*, 2009, **117**, 406–413.
- 27 Z. G. Gu, H. Fu, T. Neumann, Z. X. Xu, W. Q. Fu, W. Wenazel, L. Zhang, J. Zhang and C. Woll, *ACS Nano*, 2016, **10**, 977–983.
- 28 Z. G. Gu, Z. Chen, W. Q. Fu, F. Wang and J. Zhang, *ACS Appl. Mater. Interfaces*, 2015, **7**, 28585–28590.
- 29 C. Ohe, H. Ando, N. Sato, Y. Urai, M. Yamamoto and K. Itoh, *J. Phys. Chem. B*, 1999, **103**, 435–444.
- 30 P. Taheri, J. Wielant, T. Hauffman, J. R. Flores, F. Hannour, J. H. W. de Wit, J. M. C. Mol and H. Terryn, *Electrochim. Acta*, 2011, **56**, 1904–1911.
- 31 S. Loera-Serna, L. L. Núñez, J. Flores, R. López-Simeon and H. I. Beltrán, *RSC Adv.*, 2013, **3**, 10962–10972.
- 32 R. V. Lakshmi, T. Bharathidasan, P. Bera and B. J. Basu, *Surf. Coat. Technol.*, 2012, **206**, 3888–3894.
- 33 M. Miwa, A. Nakajima, A. Fujishima, K. Hashimoto and T. Watanabe, *Langmuir*, 2000, **16**, 5754–5760.

